

## ARTICLE

## DETECTION OF CANCER STEM CELLS MARKER IN PROSTATE CANCER USING A NANOMECHANICAL MEMBRANE-TYPE SENSOR

V. Mansouri<sup>1,2</sup>, M. Choolaei<sup>3</sup>, Y. Sefidbakht<sup>4</sup>, J. Shabani Shayeh<sup>4</sup>, Meisam Omid<sup>4\*</sup><sup>1</sup>Urogenital Stem cell research center, Shahid Beheshti University of Medical Sciences, Tehran, IRAN<sup>2</sup>Department of Basic science, Faculty of Paramedical Sciences, Shahid Beheshti University of Medical sciences, Tehran, IRAN<sup>3</sup>Research Institute of Petroleum Industry (RIPI), Tehran, IRAN<sup>4</sup>Protein Research Center, Shahid Beheshti University, GC, Velenjak, Tehran, IRAN

## ABSTRACT

In this study, we have used arrays of self-sensing piezoresistive nanomechanical membrane (NMM) to detect CD133 antigen, a protein surface marker associated with stem cells in prostate cancer. The sensing principle is based on the surface stress changes induced by antigen-antibody interaction on the NMM surfaces. NMM consists of a membrane suspended by four piezoresistive sensing components. The isotropic surface stress on the membrane results in a uniaxial stress in each sensing component, which efficiently improves the sensitivity. According to the experiments, it was revealed that NMMs have surface stress sensitivities in the order of 1.5 (mJ/m). This matter allows them to detect CD133 concentrations as low as 300 pg/ml or 150 pM. This indicates the fact that the self-sensing NMM approach is beneficial for detecting disease markers. Moreover, the performance of the NMM was compared with other detection methods and the results indicated a better performance for NMM.

## INTRODUCTION

Micro and nanofabrication technologies are new alternatives for fabricating high sensitive mechanical devices for many applications including clinical diagnosis, food quality control, and environmental monitoring [2, 3, 11]. The central element in many traditional mechanical biosensors is a small cantilever that is sensitive to the biomolecule of interest. It is possible to operate micro-cantilever sensors in two different modes, i.e. cantilever bending (surface stress method) and resonance response variation (microbalance method). In the first mode, static mode, the induced surface stress that is due to the presence of the adsorbates results in a deflection in the cantilever [26], while in the second mode, dynamic mode, the adsorbates change the resonance frequency of a cantilever due to mass loading [12].

A sensitive readout system is crucial for monitoring the deflection of cantilevers. For this reason several read-out methods have been presented. The most extended readout methods for biosensing are optical, and piezoresistive ones. The optical method is simple to implement and shows a linear response with sub-angstrom resolution, also is currently the most sensitive method. This method is employed for detecting the cantilever deflection in most studies [12, 20-22]. Nevertheless, the optical detection mechanism presents some disadvantages for example, bulky, time-consuming laser alignment on each cantilever, low applicability for large one- or two-dimensional arrays, and the difficulty of performing measurements in opaque liquids, such as blood, may hinder the potential application of this method for actual applications. The piezoresistive sensing method is known as a good alternative for the optical detection in biosensing application. The benefit of this method is that the principle works well in both liquid and gas phase and large arrays can be realized and read-out. Also, the technique is applicable for static as well as dynamic measurements [1, 9, 18, 19]. Although piezoresistive cantilevers have proven to be highly beneficial detection methods, without effective mechanical amplification schemes, their sensitivity is far below that of optical methods. In order to overcome this problem, several researches have focused on applying structural modification, such as making a through hole [18], patterning the cantilever surface [16], or variation of geometrical parameters (e.g., length, width, and overall shapes) [10, 17, 27]. Although all these methods have proven to improve the sensitivity of piezoresistive cantilevers for surface stress sensing, they have still not yielded significant stress amplification to make piezoresistive detection comparable to the optical approach, which this can be due to the fact that all these approaches rely on suppressing one of the isotropic stress components. Analytical consideration of strain amplification schemes for sensing applications based on the strategies of the constriction and double lever geometries [8, 27] has resulted in the introduction of NMMs, which have shown a considerable improvement in amplifying piezoresistive detection signals. Yoshikawa *et al*, [28] have experimentally evaluated a prototype nanomechanical membrane and the results have illustrated a significant sensitivity for piezoresistive cantilevers. In comparison with the standard piezoresistive cantilever, this study demonstrated a factor of more than 20 times higher sensitivity than that obtained with a standard piezoresistive cantilever. Presently, prostate cancer is considered as the most prevalent form of cancer in men. Recently, increasing evidence for a hierarchically organized cancer stem cell (CSC) model emerged for different tumours entities, including prostate cancer. CSCs are defined by several characteristics including self-renewal, pluripotency and tumorigenicity and are thought to be responsible for tumour recurrence, metastasis and cancer related death. A common strategy for CSC identification is flow-cytometry using assumed specific CSC surface markers, e.g., CD44 or CD166. However,

## KEY WORDS

Piezoresistive nanomechanical membrane; Cancer stem cell; CD133; Surface stress

Received: 18 July 2016  
Accepted: 15 September 2016  
Published: 5 January 2017

\*Corresponding Author  
Email:  
m\_omidi@sbm.ac.ir

many of the surface proteins used to identify CSCs are also expressed on physiological stem cells and/or progenitor cells. Human CD133 antigen, also known as AC133, was recently identified as a CSCs marker in prostate cancer [13, 24, 28]. In this work, a signal transduction biosensor has been used as a novel electrical detection for identifying CD133 marker. A direct nano-mechanical response of micro-fabricated self-sensing NMM was used to detect the surface stress changes of antigen-antibody specific binding. After injecting the CD133 target, as model biocontents, the piezoresistive responses were carefully analyzed and the feasibility of the piezoresistive membranes for biosensing were discussed in terms of device performance measures such as sensitivity, accuracy, and specificity. At the end, the results were compared with a standard cantilever.

There are very few studies regarding the wearing and laundering of lab coats in hospitals and medical practice. This study highlights the role of lab coats acting as vector for transmitting health care infections to the patients and the common areas where contamination occurs.

### Theoretical background

Molecular adsorptions on a surface do not only add mass, but also can induce surface tension or surface stress [15]. As the molecules bind, surface stress is developed – owing to electrostatic repulsion or attraction, steric interactions, hydration and entropic effects – and this can induce deflection in the mechanical element. In the piezoresistive micro/nanomechanical sensors the electrical resistivity of a piezoresistive film varies with the applied surface stress. The resistance of the silicon piezoresistor is a function of stress and the orientation of the piezoresistors. The relation between resistivity and stress can be expressed as [31]:

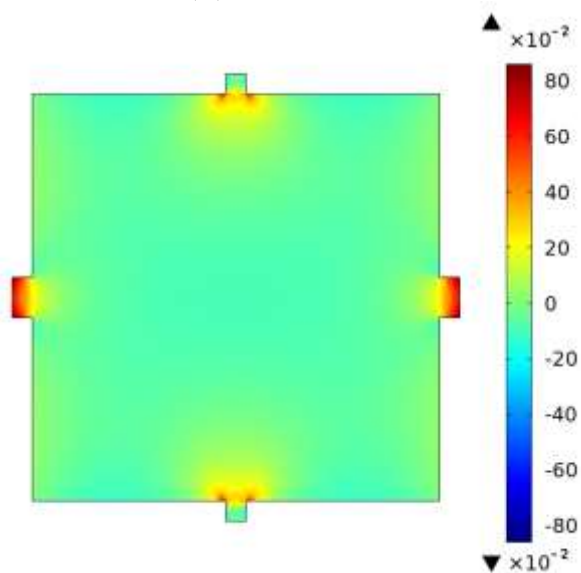
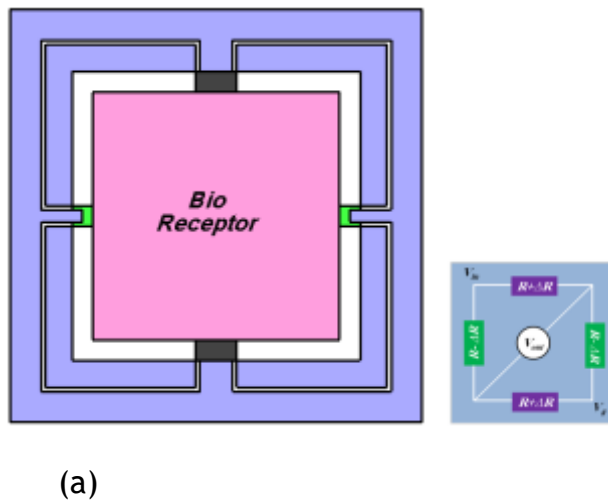


**Fig. 1: (a)** A schematic of the NMM sensor with piezoresistive sensing component (b) distribution of  $\Delta R/R$  on the surface of NMM with a dimension of  $400 \mu\text{m} \times 400 \mu\text{m} \times 2 \mu\text{m}$  when a compressive surface stress of  $-1.0 \text{ N/m}$  applied uniformly calculated by finite element analyses (FEA) using COMSOL Multiphysics 4.2.

$$\left[\frac{\Delta R}{R_0}\right] = \{\pi\}[\sigma] \quad (1)$$

where  $R_0$  is the isotropic resistivity of the unstressed crystal,  $\sigma_i$  is the stress components, and the terms  $\pi_{ij}$  the component of the piezoresistance tensor. According to equation (1), for plain stress (i.e.,  $\sigma_z = 0$ ), relative resistance change can be described as follows:

$$\frac{\Delta R}{R_0} \approx \frac{\pi_{44}}{2} (\sigma_x - \sigma_y) \quad (2)$$

From equation (2), it is clear that  $(\Delta R/R_0)$  is completely dependent on  $\sigma_x$  and  $\sigma_y$  values. In cantilevers sensors, surface stress induces an isotropic stress, and the piezoresistive signal is nearly zero except at the clamped end where the isotropic symmetry is broken. Thus, the sensor sensitivity efficiently reduces in comparison with cantilevers when a point force is applied at the free end. According to this problem NMM approach was presented by Yoshikawa et al, [28].

A simple illustration of the final NMM sensor with piezoresistive sensing component can be observed in [Fig.1a]. Owing to equation (2), isotropic surface stress leads to zero piezoresistive signal, but in the NMM structure the isotropic deformation effectively converts into a concentrated force at the connection between the membrane and the piezoresistive sensing component. [Fig. 1b] shows  $(\Delta R/R_0)$  distribution for NMM with a dimension of  $400 \mu\text{m} \times 400 \mu\text{m} \times 2 \mu\text{m}$ , when a compressive surface stress of  $-1.0 \text{ N/m}$  is applied uniformly on the NMM. COMSOL Multiphysics 4.2 finite element software was used for extracting  $(\Delta R/R_0)$  distribution. The number of elements for modeling the sensor was about 25000, which gave sufficient resolution for the present simulation.

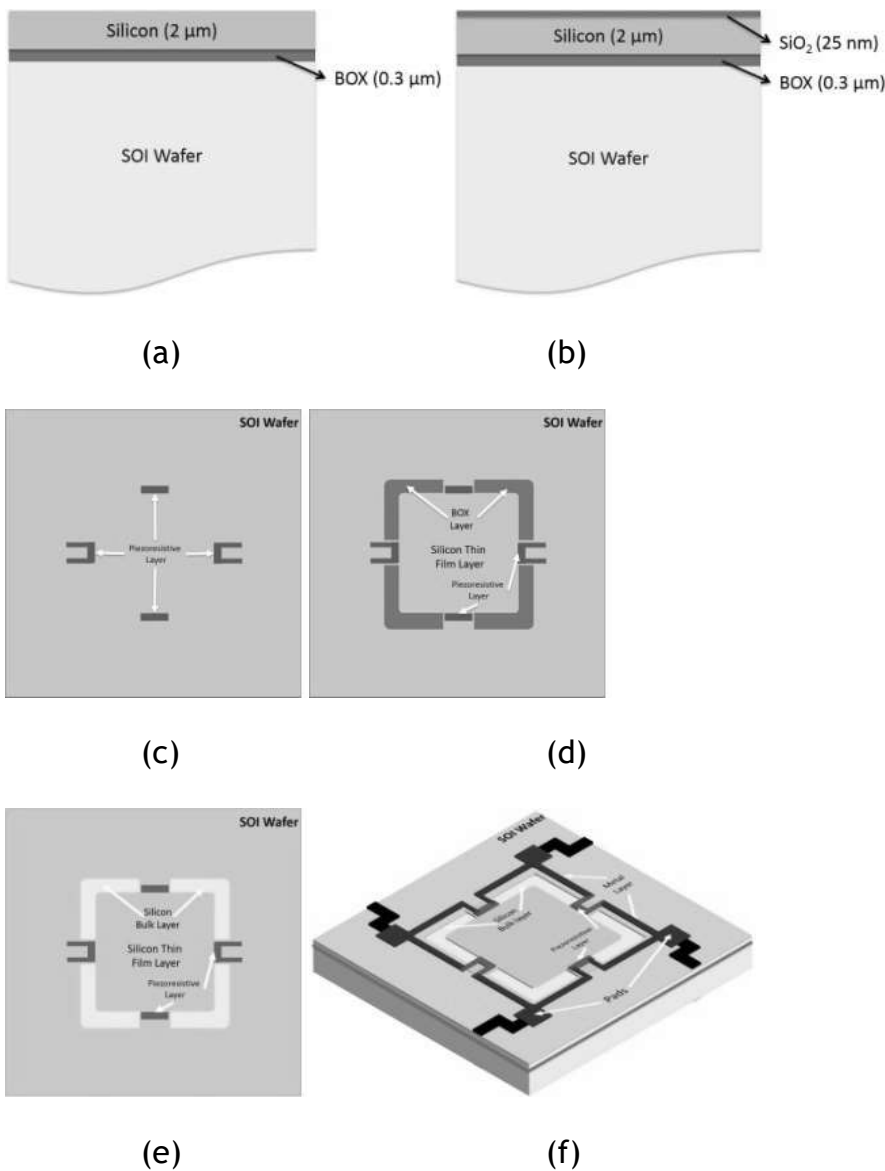
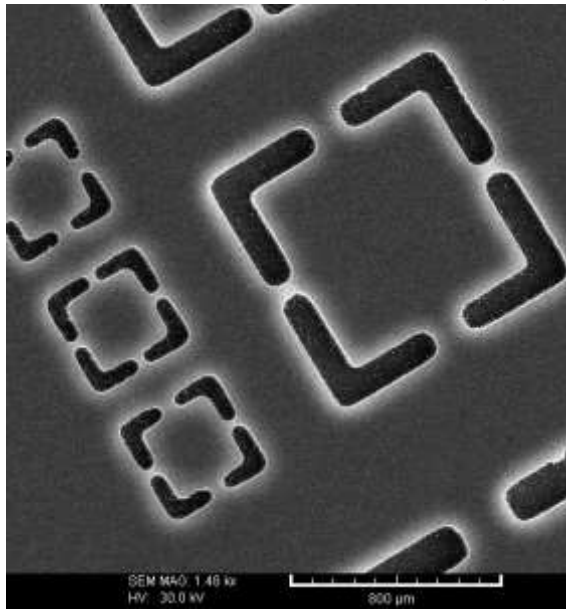


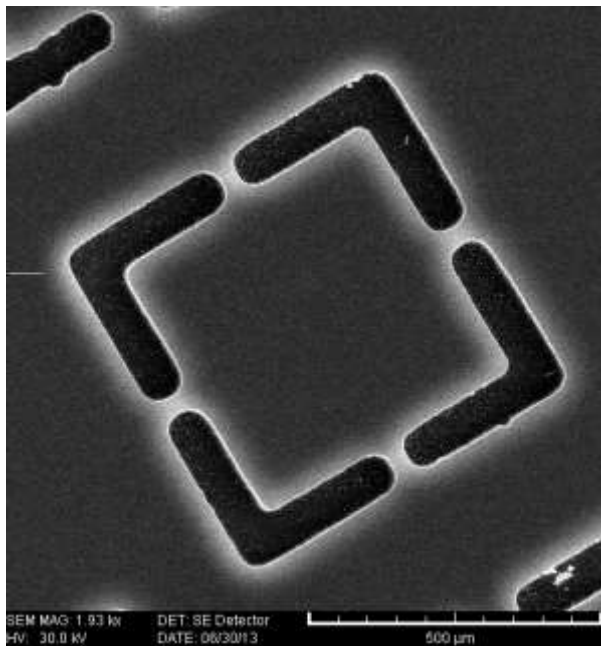
Fig. 2: Fabrication sequence of NMM.

The membrane-type geometry allows us to place a full Wheatstone bridge on the chip, when all four resistors are practically equal and the relative resistance changes are small, the total output signal  $V_{out}$  can be approximated by:

$$V_{out} = \frac{V_{in}}{4} \left( \frac{\Delta R_1}{R_1} - \frac{\Delta R_2}{R_2} + \frac{\Delta R_3}{R_3} - \frac{\Delta R_4}{R_4} \right) \quad (3)$$



(a)



(b)

**Fig. 3:** Scanning electron micrograph (SEM) of (a) NMM array chip with two different dimension of  $800 \mu\text{m} \times 800 \mu\text{m} \times 2 \mu\text{m}$  and  $400 \mu\text{m} \times 400 \mu\text{m} \times 2 \mu\text{m}$  which fabricated in a same array (b) high magnification micrograph of  $400 \mu\text{m} \times 400 \mu\text{m} \times 2 \mu\text{m}$  NMM.

According to equations (1-3), the average values of relative resistance change in the NMM has a higher value in comparison with the standard cantilever (about 43 times) [28].

The intrinsic noise level for the modified piezoresistor can be estimated by Johnson (thermal) and Hooge (1/f) noise equations [4, 5, 23]. The total intrinsic noise for NMM is reported as  $0.01\text{-}0.5 \mu\text{V}$  [7], which is still lower than the experimental noises ( $2.0\text{-}2.5 \mu\text{V}$ ), mainly caused by the electrical circuit.

## MATERIALS AND METHODS

### Fabrication of NMM sensor

We used Silicon on Insulator (SOI) wafers with a 2  $\mu\text{m}$  device layer and a 0.3  $\mu\text{m}$  buried oxide (BOX) layer as the substrate material [Fig. 2a]. Then a 25 nm silicon dioxide layer was grown by a thermal oxidation to electrically insulate the device layer from the subsequent metal layers [Fig. 2b]. The first lithographic process to define the first metal layer for electrode and sensor platform for subsequent liftoff process has been accomplished. After patterning, the photoresist, chrome (10 nm) and gold (50 nm) layers were deposited by e-beam evaporator and patterned by a liftoff process with the previously patterned photoresist [Fig. 2c]. The patterned metal layer from previous step and the patterned layer of photoresist, from the second photolithographic process were used to define the areas to be etched to define the sensor structure. The exposed device layer was etched completely by RIE to define the sensor structure. Then, a third photolithographic step for the second liftoff process, followed by the deposition of a 30-nm chrome layer and a 150-nm gold layer for wire-bonding pads. After the liftoff, a release window was photolithographically defined by the fourth lithographic process [Fig. 2d] and the exposed BOX was etched by RIE leaving the Si substrate exposed [Fig. 2e]. Then the wafer was diced into individual chips. Through the release window, the exposed Si substrate was etched by vapor phase etching using xenon difluoride ( $\text{XeF}_2$ ) to release the sensor structure. After  $\text{XeF}_2$  etching, the photoresist and the BOX were removed by BHF etching and solvent cleaning. The die was cleaned with oxygen plasma and then a 100-nm thick silicon dioxide layer was deposited with plasma enhanced chemical vapor deposition (PECVD) for insulation. Chrome (20 nm) and gold (50 nm) layers were deposited using an e-beam evaporator for an immobilization layer for protein-protein interaction. The PECVD oxide on the bonding pads was selectively etched for wire-bonding. Then each die was attached to a custom made printed circuit board (PCB) and was wire-bonded. [Fig. 3] presents the final picture of NMMs in different sizes fabricated in the same array using a Scanning electron micrograph (SEM).

### CD133 antibody immobilization process

A fresh piranha solution (a 4:1 ratio of  $\text{H}_2\text{SO}_4$  (98.08%) and  $\text{H}_2\text{O}_2$  (34.01%)) was used to wash and clean the membranes, in order to remove experimental contamination of the Au surface. After 1 min, the membranes were taken out of the solution and were rinsed using deionized water. To complete the cleaning process, the rinsed membranes were dried using a stream of  $\text{N}_2$  gas. For 2 h at room temperature in darkness a 0.1 M deoxygenated cysteamine (Sigma, 95%) aqueous solution was used to functionalize the devices. Then, NMMs were washed with deionized water and soaked in water for 12 h to remove the physically adsorbed cysteamine. Moreover, for creating a covalent cross-linker molecule between the amine groups on the NMM surface and antibodies, chips were soaked in a 5% solution of glutaraldehyde (Sigma, 50%) in borate buffer for 2 hours. Following this and all subsequent steps, device chips were washed twice, each washing step was for two minutes, in purified DI water on an orbital shaker operating at 95 RPM. It should be mentioned that fresh water was used between washes. The reason of using water instead of buffer for washing was to prevent the abundant formation of buffer salt crystals on the surface of devices which make the sensors effectively useless.

Next, one hour incubation was used to immobilize the monoclonal anti-CD133 (Fitzgerald Industries International Inc., Concord, MA, USA), affinity-purified, with a concentration of 50 mg/mL on the surface. By immersing the NMM in 50 mM solution of glycine for 30 minutes unreacted glutaraldehyde was then quenched. In addition, dissolved bovine serum albumin (BSA, Sigma, St. Louis, MO, USA) in phosphate buffered saline (PBS) with 10 mg/ml concentration was used to prevent non-specific binding. For this purpose, the membranes were immersed in this solution for 1 h at room temperature. Then, they were rinsed with PBS (pH 7.4) containing polyoxyethylenesorbitan monolaurate (Tween 20, St. Louis, MO, USA) and finally washing was performed by only using PBS solution.

### Electrical measurements

For the electrical measurement of sensor, internal dc-bias Wheatstone bridge was used. A bridge supply voltage of 1.5V was applied using a dc power supply (Agilent, E3631A), and the sensor output voltage was measured by a multimeter (Keithley, 2010 7-1/2). Moreover, a Faraday cage was adopted for noise reduction. The above components were used to measure the piezoresistive response of the NMM in a liquid environment.

## RESULTS AND DISCUSSION

In order to reach results with high reliability, the surfaces of the membranes were stabilized by treating them with a PBS buffer. The PBS buffer was directed with a typical flow rate of 0.4 – 0.5 ml/hour, for 1 h, to the NMM sensor arrays using a flexible PDMS polymer microfluidic channel sealed to the device chip.

As a general trend, at the point of initial injection of the PBS buffer the induced voltage of the NMM increased rapidly and steadily decreased with time, which in this case the induced voltage of the NMM reached dynamic equilibrium after 10 min. For the bio-assay, CD133 antigens were injected into each liquid chamber, including the stabilized membrane. The liquid temperature was precisely controlled and external noise sources were excluded using a shield box. In order to estimate the nonspecific adsorption on the NMM surface, the concentration of BSA in all solutions was stabilized at 0.1 mg/ml.

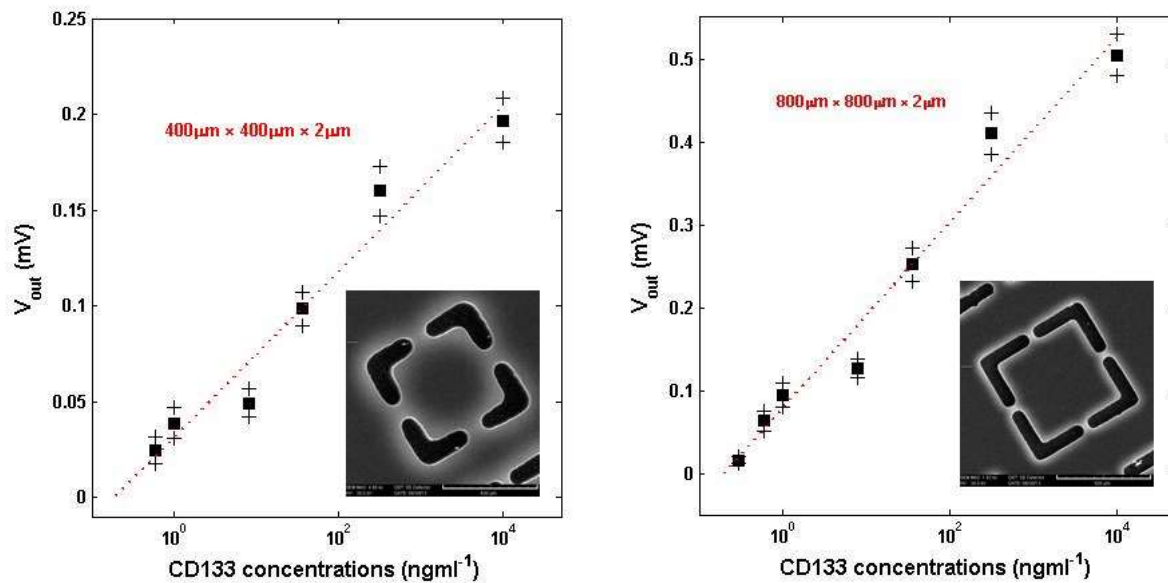


**Fig. 4:** Steady-state output signals ( $V_{out}$ ) as a function of CD133 concentrations for two different NMM geometries. Every data point on this plot represents an average of output signals obtained in multiple experiments done with different NMM, whereas the range of output signals obtained from these experiments is shown as the error bar.

[Fig. 4] shows the steady-state output signals ( $V_{out}$ ) as a function of CD133 concentration in a BSA background for different dimensions of NMM. By using a  $400\ \mu\text{m} \times 400\ \mu\text{m} \times 2\ \mu\text{m}$  NMM, the lowest CD133 concentration that we could clearly detect above noise was  $0.6\ \text{ng/ml}$ . However, when a  $800\ \mu\text{m} \times 800\ \mu\text{m} \times 2\ \mu\text{m}$  NMM was used, CD133 concentration as low as  $0.3\ \text{ng/ml}$  was detectable. The experimental results presented a range of linearity of  $0.3\ \text{ng/ml}$  to  $10\ \mu\text{g/ml}$  and  $0.6\ \text{ng/ml}$  to  $10\ \mu\text{g/ml}$  for  $800\ \mu\text{m} \times 800\ \mu\text{m} \times 2\ \mu\text{m}$  and  $400\ \mu\text{m} \times 400\ \mu\text{m} \times 2\ \mu\text{m}$  NMM, respectively. The minimum detectable surface stress for each sensor can be obtain when the output signals are equal to the noise values. By using the experimental results,  $1.5$  and  $2.5\ \text{mJ/m}$  were respectively the minimum surface stress sensitivities for the  $800\ \mu\text{m} \times 800\ \mu\text{m} \times 2\ \mu\text{m}$  and  $400\ \mu\text{m} \times 400\ \mu\text{m} \times 2\ \mu\text{m}$  NMM. In order to check the sensitivity of the present NMM -based biosensor, the results have been compared with other label free biosensing technologies. In Table 1, the minimum detection limits (LOD) of NMMs with different dimensions have been compared with a standard cantilever (MCL) [4-14], surface-plasmon resonance (SPR) [6], quartz crystal monitor (QCM) [30], and electrochemical [29] sensors. In most cases the NMM -based biosensor has the lowest LOD. Results indicate that NMM has comparable sensitivity with the optical read-out methods, moreover its sensitivity is significantly higher than a standard piezoresistive cantilever. This table quite well reflects the potential of the NMM -based biosensor in the pharmaceutical and medical diagnosis fields.

**Table 1:** The minimum limit of detection (LOD) of biomarker by different biosensors

(a)  $400\ \mu\text{m} \times 400\ \mu\text{m} \times 2\ \mu\text{m}$ .

Category	Detection conditions	LOD
NMM	0.1 mg/ml BSA	$0.6\ \text{ng/ml}$ <sup>(a)</sup>
	0.1 mg/ml BSA	$0.3\ \text{ng/ml}$ <sup>(b)</sup>
MCL [30]with reference cantilever, piezoresistive detection	0.1 mg/ml BSA	$10\ \text{ng/ml}$
MCL [4] no reference cantilever, optical detection	$1.0\ \text{mg/ml}$ HSA	$0.2\ \text{ng/ml}$
SPR [25] Direct immunoassay	$0.3\ \text{mg/ml}$ BSA	$300\ \text{ng/ml}$
QCM [28] Direct assay based on yeast cells strategy	serum	$5\ \text{ng/ml}$
Electrochemical [14] Amperometric Sandwich immunoassay	phosphate buffer	$0.25\ \text{ng/ml}$

(b)  $800\ \mu\text{m} \times 800\ \mu\text{m} \times 2\ \mu\text{m}$ .

## CONCLUSION

We have reported a novel signal transduction biosensor for detecting CD133, using a unique micro-fabricated self-sensing array of NMM sensors. Unlike cantilever sensors, which are based on optical readout systems, the NMM integrated piezoresistive readout sensors facilitate the detection of compact devices in even non-transparent environments. In comparison with traditional piezoresistive based cantilever sensors [9-16-20], our unique NMM design significantly improves sensor sensitivity that allows us to detect CD133 concentrations as low as 300 pg mL<sup>-1</sup>, or 150 pM.

### CONFLICT OF INTEREST

There is no conflict of interest.

### ACKNOWLEDGEMENTS

None

### FINANCIAL DISCLOSURE

None

## REFERENCES

- [1] Aeschimann L, Meister A, Akiyama T, Chui B W, Niedermann P, Heinzelmann H, De Rooij N, Stauer Urs Vettiger P. [2006] Scanning probe arrays for life sciences and nanobiology applications. *Microelectronic Engineering*. 83(4): 1698-1701.
- [2] Alvarez M, Lechuga L M. [2010] Microcantilever-based platforms as biosensing tools. *Analyst*. 135(5): 827-836.
- [3] Baniasadi L, Omidi M, Amoabediny Gh, Yazdian F, Attar H, Heydarzadeh A, Zarami A, Hatamian Sheikhha M. [2014] An inhibitory enzyme electrode for hydrogen sulfide detection. *Enzyme and microbial technology*. 63: 7-12.
- [4] Berger R, Delamar E, Lang Hans P, Gerber C, Gimzewski J K, Meyer E . [1997] Surface stress in the self-assembly of alkanethiols on gold. *Science*. 276(5321): 2021-2024.
- [5] Dohn S, Sandberg R, Svendsen W, Boisen A. [2005] Enhanced functionality of cantilever based mass sensors using higher modes. *Applied Physics Letters*. 86(23): 233501.
- [6] Harkey JA, Kenny T W. [2000] 1/f noise considerations for the design and process optimization of piezoresistive cantilevers. *Journal of Microelectromechanical Systems*. 9(2): 226-235.
- [7] Hooge Friits N, 1969, 1/f noise is no surface effect. *Physics letters A*. 29(3): 139-140.
- [8] Shabani Shayeh J , Norouzi P, Ganjali M. [2016] Effect of Thickness on the Capacitive Behavior and Stability of Ultrathin Polyaniline for High Speed Super Capacitors. *Russian Journal of Electrochemistry*. 52(10): 933-937.
- [9] shabani shayeh J, Ranaei Siadat S O, \Sadeghnia M, niknam K, Rezaei M. Ahgamohammadi N. [2016] Advanced studies of coupled conductive polymer/metal oxide nano wire composite as an efficient supercapacitor by common and fast Fourier electrochemical methods. *Journal of Molecular liquids*. 220(1): 489-494.
- [10] Loui A, Goericke FT, Ratto TV, Lee J, Hart BR King WP. [2008] The effect of piezoresistive microcantilever geometry on cantilever sensitivity during surface stress chemical sensing. *Sensors and Actuators A: Physical*. 147(2): 516-521.
- [11] Omidi M, Alaie S Rousta A. [2012] Analysis of the vibrational behavior of the composite cylinders reinforced with non-uniform distributed carbon nanotubes using micro-mechanical approach. *Meccanica*. 47(4): 817-833.
- [12] Omidi M, Malakoutian MA, Choolaei M, Oroojalian F, Haghirsadat F, Yazdian F. [2013] A Label-Free Detection of Biomolecules Using Micromechanical Biosensors. *Chinese Physics Letters*. 30(6): 068701.
- [13] Park K, Millet L J, Kim N, Li H, Jin X, Popescu G, Aluru NR, Hsia K J, Bashir R. [2010] Measurement of adherent cell mass and growth. *Proceedings of the National Academy of Sciences*. 107(48): 20691-20696.
- [14] Partin Alan W, Catalona William J, Southwick Paula C, Subong Eric NP, Gasior Gail H Chan Daniel W. [1996] Analysis of percent free prostate-specific antigen (PSA) for prostate cancer detection: influence of total PSA, prostate volume, and age. *Urology*. 48(6): 55-61.
- [15] Polascik T J, OESTERLING J, PARTIN A. [1999] Prostate specific antigen: a decade of discovery-what we have learned and where we are going. *The Journal of urology*. 162(2): 293-306.
- [16] Privorotskaya N, King William. [2009] The mechanics of polymer swelling on microcantilever sensors. *Microsystem Technologies*. 15(2): 333-340.
- [17] Rahimpour A, Yazdian F, Akbari Z, Rajabibazl M, Meisam O. [2016] Design and Manufacturing of Electromechanical Chip for Rapid Measurement of IgG1 Antibody in Cell-Culture Supernatant. *Biology and Medicine*.
- [18] Rashidi A, Omidi M, Choolaei M, Nazarzadeh M, Yadegari A, Haghierosadat F, Oroojalian F, Azhdari M. [2013] Electromechanical properties of vertically aligned carbon nanotube. in *Advanced Materials Research*. Trans Tech Publ.
- [19] Salehifar N, Shabani Shayeh J, Ranaei Siadat S O, Niknam K, Ehsani A, Kazemi Movahhed S. [2015] Electrochemical study of supercapacitor performance of polypyrrole ternary nanocomposite electrode by fast Fourier transform continuous cyclic voltammetry. *RSC Advances*. 5(116): 96130-96137.

- [20] Shabani Shayeh J, Ehsani A, Ganjali M R, Norouzi P, Jaleh B. [2015] Conductive polymer/reduced graphene oxide/Au nano particles as efficient composite materials in electrochemical supercapacitors. *Applied Surface Science*. 353: 594-599.
- [21] Shabani Shayeh J, Ehsani A, Nikkar A, Norouzi P, Ganjali M, Wojdyla M. [2015] Physioelectrochemical investigation of the supercapacitive performance of a ternary nanocomposite by common electrochemical methods and fast Fourier transform voltammetry. *New Journal of Chemistry*. 39: 9454-9460.
- [22] Thundat T, Warmack R Js, Chen GY, Allison DP. [1994] Thermal and ambient-induced deflections of scanning force microscope cantilevers. *Applied Physics Letters*. 64(21): 2894-2896.
- [23] Tufte ON, Stelzer EL. [1963] Piezoresistive properties of silicon diffused layers. *Journal of Applied Physics*. 34(2): 313-318.
- [24] Waggoner JW, Löest CA, Turner JL, Mathis CP, Hallford DM. [2009] Effects of dietary protein and bacterial lipopolysaccharide infusion on nitrogen metabolism and hormonal responses of growing beef steers. *Journal of animal science*. 87(11): 3656-3668.
- [25] Woodrum D, Brawer M, Partin A, Catalona W, Southwick P. [1998] Interpretation of free prostate specific antigen clinical research studies for the detection of prostate cancer. *The Journal of urology*. 159(1): 5-12.
- [26] Wu G, Datar R, Hansen K, Thundat T, Cote R, Majumdar A. [2001] Bioassay of prostate-specific antigen (PSA) using microcantilevers. *Nature biotechnology*. 19(9): 856-860.
- [27] Yang Shih-Ming, Yin TI, Chang C. [2007] Development of a double-microcantilever for surface stress measurement in microsensors. *Sensors and Actuators B: Chemical*. 121(2): 545-551.
- [28] Yoshikawa G, Akiyama T, Gautsch S, Vettiger P, Rohrer H. [2011] Nanomechanical membrane-type surface stress sensor. *Nano letters*. 11(3): 1044-1048.
- [29] Yoshikawa G, Akiyama T, Loizeau F, Shiba K, Gautsch S, Nakayama T, Vettiger P, Rooij Nico F, de Aono M. [2012] Two dimensional array of piezoresistive nanomechanical membrane-type surface stress sensor (MSS) with improved sensitivity. *Sensors*. 12(11): 15873-15887.
- [30] Yu X, Thaysen J, Hansen O, Boisen A. [2002] Optimization of sensitivity and noise in piezoresistive cantilevers. *Journal of Applied Physics*. 92(10): 6296-6301.
- [31] Zhou Y, Larsen P, Hao C, Yong W. [2002] CXCR4 is a major chemokine receptor on glioma cells and mediates their survival. *Journal of Biological Chemistry*. 277(51): 49481-49487.